water

MDPI

Article

Satellite Estimation of Chlorophyll-a Using Moderate Resolution Imaging Spectroradiometer (MODIS) Sensor in Shallow Coastal Water Bodies: Validation and Improvement

Mohd Manzar Abbas, Assefa M. Melesse *, Leonard J. Scinto and Jennifer S. Rehage

Department of Earth and Environment, Florida International University, Miami, FL 33199, USA
* Correspondence: melessea@fiu.edu

Received: 15 May 2019; Accepted: 30 July 2019; Published: 6 August 2019

Abstract: The size and distribution of Phytoplankton populations are indicators of the ecological status of a water body. The chlorophyll-a (Chl-a) concentration is estimated as a proxy for the distribution of phytoplankton biomass. Remote sensing is the only practical method for the synoptic assessment of Chl-a at large spatial and temporal scales. Long-term records of ocean color data from the MODIS Aqua Sensor have proven inadequate to assess Chl-a due to the lack of a robust ocean color algorithm. Chl-a estimation in shallow and coastal water bodies has been a challenge and existing operational algorithms are only suitable for deeper water bodies. In this study, the Ocean Color 3M (OC3M) derived Chl-a concentrations were compared with observed data to assess the performance of the OC3M algorithm. Subsequently, a regression analysis between in situ Chl-a and remote sensing reflectance was performed to obtain a green-red band algorithm for coastal (case 2) water. The OC3M algorithm yielded an accurate estimate of Chl-a for deep ocean (case 1) water (RMSE = 0.007, r^2 = 0.518, $p < 0.001$), but failed to perform well in the coastal (case 2) water of Chesapeake Bay (RMSE = 23.217, r^2 = 0.009, p = 0.356). The algorithm developed in this study predicted Chl-a more accurately in Chesapeake Bay (RMSE = 4.924, r^2 = 0.444, $p < 0.001$) than the OC3M algorithm. The study indicates a maximum band ratio formulation using green and red bands could improve the satellite estimation of Chl-a in coastal waters.

Keywords: chlorophyll-a; algal bloom; Chesapeake Bay; ocean color algorithm; coastal water; MODIS

1. Introduction

Phytoplankton are micro-autotrophs that play a major role in primary production and oxygen generation in aquatic systems. However, a disproportional increase in phytoplankton biomass may result in algal blooms. There are certain species of phytoplankton that produce bio-toxins (e.g., *Karenia brevis*) [1,2]. Proliferation of these species, also called harmful algal blooms (HAB), causes serious impact on marine and human health [1]. Nutrient inputs from contributing watersheds and rivers have been shown to be responsible for the accelerated eutrophication of receiving water bodies [3,4]. The problem of algal bloom is expected to worsen with global climate change [5]. Understanding the dynamics of phytoplankton populations and their distribution enables assessment of the nutrient state, health, and ecological integrity of a body of water. Since chlorophyll-a (Chl-a) exists in every species of phytoplankton [6], its concentration is used as a proxy for the distribution of phytoplankton biomass [7,8]. The conventional method of Chl-a estimation requires water sample collection and laboratory analysis [9]. This method, effort-intensive and time consuming, is unsuitable for large spatio-temporal scales. Instead, satellite-based sensors can be used for the synoptic assessment of Chl-a at large spatial scales. The launch of the first satellite borne ocean color sensor, the Coastal Zone

Color Scanner (CZCS), in 1978, began an evolution of satellite deployments with improved sensors, higher precision, and an increased number of spectral bands [10]. Currently, one operational ocean color sensor, Moderate Resolution Imaging Spectroradiometer (MODIS) Aqua, collects data with 1–2 days of temporal resolution. The default Chl-a retrieving algorithm for MODIS Aqua, the Ocean Color 3M (OC3M) algorithm, is a blue-green band ratio algorithm [11].

In spite of the development of advanced and precise sensors, the error in the satellite estimation of Chl-a concentration in coastal waters is high [12]. This can be due to the bottom reflectance in shallow water systems. Researchers have classified the ocean water areas as case 1 and case 2 water. The optical property of the surface of deep ocean water is dominated by phytoplankton and is termed as case 1 water [13]. In coastal regions, the optical property of water is influenced by colored dissolved organic matter (CDOM), bottom reflectance, and total suspended matter (TSM), and is referred to as case 2 water. The blue-green band ratio strongly correlates to Chl-a concentration in case 1 water, however, in case 2 waters, the correlation becomes weak [14]. Furthermore, because of a low attenuating tendency, the green band is heavily influenced by bottom reflectance in shallow coastal water [15]. The OC3M algorithm that uses the blue-green band ratio has been shown to yield accurate results in case 1 waters [16]. However, the algorithm overestimates the Chl-a in case 2 waters [12].

Over 50% of the world's population lives in coastal zones [17], and coastal waters provide many ecosystem services of human importance including fisheries and recreation. Primary production in coastal areas influences fisheries, eutrophication, and algal blooms that affect human populations. Ocean color data from a satellite-based sensor are the only practical tools for the global assessment of spatiotemporal variation in phytoplankton populations. The long record of MODIS ocean color data of coastal regions currently cannot be utilized due to a lack of a precise algorithm for the Chl-a estimation. A robust algorithm would make use of all available data and will have a significant effect on the understanding of various factors that regulate primary production in ocean water. Furthermore, precise assessment of phytoplankton biomass will assist in understanding models of atmospheric carbon dioxide flux to the ocean, and the influence of anthropogenic contaminants on the marine ecosystem [9].

The red band has a tendency of attenuating within surface water depths, and therefore is less affected by bottom reflectance [15]. Furthermore, it is less sensitive to CDOM [18]. Therefore, red bands have been used in several studies to develop Chl-a algorithm for shallow coastal water [15,16,19–21]. In such algorithms, the green band or near-infrared (NIR) band are commonly used in combination with red band [15,16,19–21]. Gons, et al. [22] used an algorithm based on backscattering coefficients at NIR bands to retrieve the Chl-a concentration. Gilerson, et al. [18] used an algorithm based on the ratio of a red to NIR band. Gitelson, et al. [23] and Le, et al. [24] demonstrated the applicability of red-NIR algorithms in estuarine water, including the Chesapeake Bay. Blakey, et al. [25] developed the Benthic Class Specific algorithm to reduce the noise due to bottom reflectance. However, these algorithms have a limited application. Processed data with atmospheric correction are not provided for NIR bands as part of the standard data suite. Applicability of the Benthic Class Specific Algorithm is contingent on the availability of Sea Grass Density data at the location. To utilize the abundance of MODIS ocean color data of coastal regions, an improved algorithm is required that will use the wave bands for which MODIS reflectance data are available.

MODIS Aqua's level-2 data suit provides processed reflectance data in blue, green and red bands. Therefore, many algorithms have been developed for MODIS sensor using green and red bands, and have been shown to perform better than the OC3M algorithm but significant inaccuracy in estimation using these algorithms leaves the scope for further improvement [19–21]. A green-red band ratio algorithm is based on the fact that Chl-a reflects radiation in green band whereas absorbs radiations in the red band resulting in a reflectance peak in the green region and reflectance trough in the red region of the spectrum [14]. Schalles, et al. [14] in his mesocosm experiment demonstrated the wavelength position of the green peak shifts towards the higher wavelength as the Chl-a concentration increases. Similarly, the trough observed in red band shifts from lower band to higher band as the

Chl-a concentration increases. Therefore, instead of using the ratio of reflectance at one wavelength, each from green and red bands, an algorithm that employs the ratio of maximum reflectance in green band to minimum reflectance in red band could further improve the satellite estimation of Chl-a in the coastal water (case 2) by more efficiently targeting the peak and trough, and increasing the reflectance ratio.

In this study, the performance of the OC3M algorithm in case 1 and case 2 waters was assessed, and an algorithm was developed for case 2 water, using an alternative band combination from the green-red wavebands of the MODIS Aqua sensor. Since the algorithm utilizes four bands from the green and red region of the spectrum, it has been named as Green-Red Ocean Color 4 algorithm (here after GROC4). The performance of the GROC4 algorithm was tested and compared with that of the OC3M and other green-red algorithms using an independent dataset, and finally the seasonal performance of the GROC4 was evaluated. Thus, the specific objectives of this study were to (1) evaluate the performance of the OC3M model in case 1 and case 2 waters, (2) develop an improved Chl-a estimation algorithm for case 2 water, and (3) evaluate the performance of the newly developed model in case 2 water with seasonal data.

2. Materials and Methods

2.1. Study Area

The shallow water system of Chesapeake Bay (Figure 1) was chosen as the study area for the validation of OC3M algorithm in case 2 water and the development of an improved algorithm. Chesapeake Bay is the largest estuary in North America, located along the United States east coast, lying inland from the Atlantic Ocean. Importantly, the Bay also has a rich Chl-a dataset to test and validate the models for case 2 water.

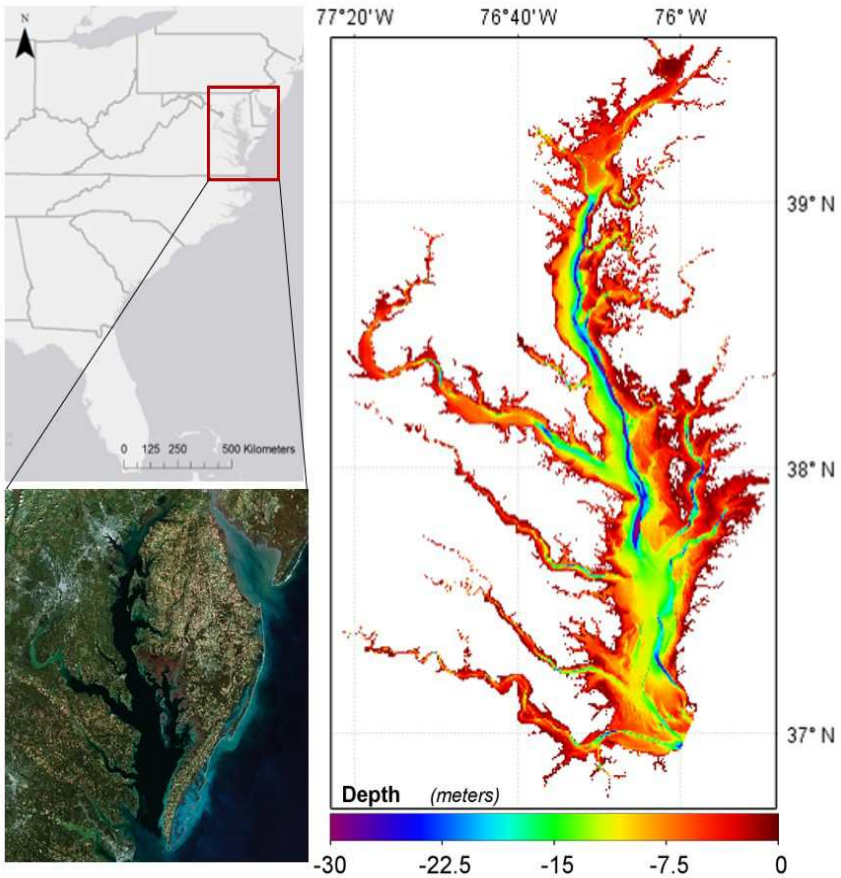

Figure 1. Map showing the location and bathymetry of Chesapeake Bay.

The Chesapeake Bay watershed extends to an area of more than 102,400 km^2 that covers parts of Delaware, Maryland, New York, Pennsylvania, Virginia, and West Virginia. The bay is classified as a highly productive water system [26]. The high productivity is associated with excessive nutrients carried into the bay water through river discharge [27]. The Chesapeake Bay watershed receives a high volume of precipitation (1250 mm annually) that generates an annual run-off equivalent to 400 mm.

More than 150 streams and rivers flow into the Chesapeake Bay watershed. Major rivers that drain into the bay include the Susquehanna, James, York, Rappahannock, Potomac from the west, and the Wicomico, Nanticoke and Choptank from the east. The main source of freshwater inflow in Chesapeake Bay is the Susquehanna River, responsible for about 50% of the total inflow. The Susquehanna and Potomac Rivers carry 62% of the Nitrogen and 44% of the Phosphorus flux to the bay water [28]. Agricultural activities are common in the Chesapeake Bay watershed, with more than 25% of watershed area is utilized for agricultural activities. Runoff from agricultural lands is the major source of Nitrogen (54%) and Phosphorus (43%) loading in the Bay [28]. The eastern shore of the bay inputs a disproportionally high amount of nutrients from agricultural fertilizers. In 2001, 49% of land area in this region was used for agriculture [27]. Soils and sediments in the region are sandy and permeable, promoting the movement of nutrients from source to streams and tidal waters [27].

The accuracy of satellite estimation of Chl-a in the coastal region is associated with depth of the water [29], which is correlated with distance to shore. Therefore, the availability of long-term in situ Chl-a concentration data at varying distances from the coast with diverse bathymetry makes Chesapeake Bay a suitable study area for the development of an ocean color algorithm. The complex bio-optical property of Chesapeake Bay's water is dominated by colored dissolved organic matter (CDOM), total suspended sediments (TSS) and phytoplankton [30]. The Chesapeake Bay experiences frequent algal blooms and hypoxic conditions [31]. The bay is a major economic resource for the region, and associated economic activities (fishing, tourism etc.) are highly dependent on water quality. Considering the economic importance of the bay and its deteriorating condition, a major restoration project is underway [26].

The Sargasso Sea, located in the Atlantic Ocean (Figure 2), was selected as the study area for the validation of OC3M algorithm in case 1 water. The study area is an oligotrophic ocean gyre, which is bound by a clockwise flow of ocean currents [32]. The mean annual Chl-a concentration in Sargasso Sea is reported to be less than 0.05 mg m^{-3} [33]. A spring bloom is a seasonal phenomenon in the region that occurs from March to April due to warm surface water [34].

2.2. In Situ Data

The field-measured Chl-a data of Chesapeake Bay, along with sampling dates and coordinates of the sampling locations, were downloaded from the Chesapeake Bay Program (CBP) website [35]. The CBP provides a long record of Chl-a concentration data of the bay water at spatially diverse locations. In situ observations from 2012 to 2017 were used to obtain observed and remote sensing matchup pairs (see details below). Data from 2012 to 2016 were used for the validation of OC3M algorithm and development of the GROC4 algorithm; whereas 2017 data were used to validate the GROC4 algorithm and analyze its seasonal performance.

In situ Chl-a data for Sargasso Sea were obtained from the National Centre for Environmental Information (NCEI) database for validation of OC3M algorithm in case 1 water [36]. Chl-a samples were collected by the National Science Foundation (NSF) owned research vessel, Oceanus, in 2004 and 2005. Figure 2 shows the sampling locations in Chesapeake Bay and Sargasso Sea. A summary of in situ data used in this study is presented in Table 1.

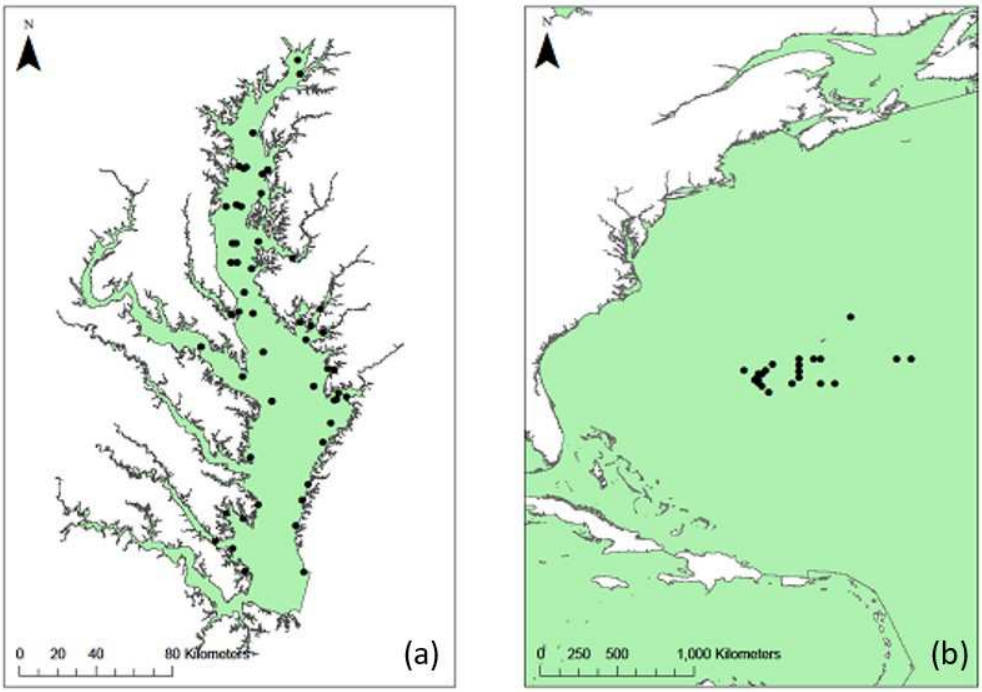

Figure 2. Map showing the locations of Chl-a in situ measurements used in our study. (**a**) Monitoring stations used for the validation of the Ocean Color 3M (OC3M) algorithm in Chesapeake Bay, and development of the GROC4 algorithm and (**b**) Sampling locations in the Sargasso Sea, Atlantic Ocean.

Table 1. Summary of in situ Chl-a data used in this study.

Location	Purpose	Sampling Locations	Samples	Period	Chl-a (mg m^{-3})		
					Max	Min	Mean
Chesapeake Bay	Validation of the OC3M and development of the GROC4 algorithm	47	134	2012–16	71.782	2.674	16.462
	Validation of the GROC4 algorithm	38	110	2017	38.021	1.736	10.698
Sargasso Sea	Validation of the OC3M Algorithm	25	25	2004–05	0.062	0.030	0.047

2.3. Satellite Data

Remote sensing reflectance data from the MODIS Aqua sensor were used for this study. MODIS Aqua acquires remote sensing data in 36 spectral bands. The swath width of viewing is 2330 km allowing MODIS cover to the entire Earth in 1–2 days. The spatial resolutions of MODIS bands are 250, 500 or 1000 m. Out of the 36 bands, 10 bands are useful for ocean color studies, with a spatial resolution of 1000 m.

The Ocean Biology Processing Group (OBPG) located at NASA's Goddard Space Flight Centre, manages Ocean Color Web (OCW), and collects, validates, archives and distributes ocean-related remote sensing data. The MODIS Aqua's ocean color level-2 data were downloaded for Chesapeake Bay (2012–2017) and Sargasso Sea (2004–2005) from OCW using the level-2 data browser [37]. The level-2 data contains atmospherically corrected raster images of reflectance values at available bands. Swaths that contain the study area (Chesapeake Bay or Sargasso Sea), and dates for which in situ data is available were the criteria for inclusion in our study.

2.4. Extraction of In Situ-Satellite Matchup Pairs

Level-2 MODIS Aqua data were searched to find data associated with each in situ sampling points. An in situ observation and a single pixel of remote sensing data, covering the in situ sampling location, were considered as a match-up pair. Pixels flagged for stray light, land, cloud, sun glint, high top-of-atmosphere and atmospheric correction failure were excluded as in Bailey and Werdell [38]. A total of 269 match-up pairs were extracted of which 244 were for Chesapeake Bay and 25 for the Sargasso Sea.

2.5. Validation of the Ocean Color 3M (OC3M) Algorithm

Ocean color algorithms derive Chl-a concentration of a water body using remote sensing data. O'Reilly et al. (1998) developed an ocean color algorithm (i.e., OC4) for SeaWiFS that uses the ratio of reflectance in blue to green bands [10]. The Ocean Color 3M (OC3M) algorithm currently operational for MODIS is an extension of the OC4 algorithm that has been modified according to MODIS bands. The OC3M algorithm is a polynomial relationship of the fourth order between Chl-a concentration and reflectance ratio that takes reflectance at 443, 488 and 547 nm as input and gives Chl-a concentration in mg m^{-3} as output (Equations (1) and (2)).

$$\text{Chl-a} = 10^{a0 + a1 \times X + a2 \times X^2 + a3 \times X^3 + a4 \times X^4} \tag{1}$$

$$X = log_{10} \frac{\lambda_b}{\lambda_g} \tag{2}$$

where, λ_b is the greater of remote sensing reflectance (R_{rs}) at 443 and 488, and λ_g is R_{rs} at 547. The a0, a1, a2, a3 and a4 are constants whose values are 0.2424, −2.7423, 1.8017, 0.0015 and −1.2280, respectively.

The present study analyzed the performance of the OC3M algorithm in Sargasso Sea (case 1) and Chesapeake Bay (case 2) water. The OC3M algorithm was applied to the remote sensing pixels and algorithm-derived concentrations were compared with the corresponding in situ measurements. The SeaDAS 7.4 software, a software package for analysis of remote sensing ocean color data, was used. Finally, the overall performances of the algorithm in Sargasso Sea and Chesapeake Bay were compared. Statistical parameters including Root Mean Square Error (RMSE), Mean Absolute Percent Error (MAPE) and Mean Absolute Error (MAE) were derived to examine the accuracy of the OC3M algorithm in Sargasso Sea and Chesapeake Bay. The following equations were used to calculate these statistical parameters:

$$\text{RMSE} = \sqrt{\frac{\sum_{i=1}^{n} (X - Y)^2}{n}} \tag{3}$$

$$\text{MAE} = \frac{\sum_{i=1}^{n} |X - Y|}{n} \tag{4}$$

$$\text{MAPE} = \frac{100}{n} \sum_{i=1}^{n} \left| \frac{X - Y}{X} \right| \tag{5}$$

where, X = In situ measurements, Y = Algorithm-derived values and n = Number of samples.

2.6. The Green-Red Ocean Color 4 (GROC4) Algorithm

An improved algorithm (GROC4) for case 2 water was developed using remote sensing reflectance in green and red bands. To develop the algorithm, the ratio of maximum reflectance in the green band and minimum reflectance in the red band was used, targeting the peak reflectance in green band and the trough in the red band. Regression analysis was performed between logarithmic reflectance ratios and logarithmic in situ Chl-a concentrations, employing the matchup pixels to generate coefficients for a fourth-order polynomial used in the algorithm.

2.7. Validation of the GROC4 Algorithm

The GROC4 algorithm developed in this study was validated by using an independent test sample consisting of 110 pairs of match-up data. These match-up pairs were not used in the development of the algorithm. The algorithm-derived concentrations were compared with the corresponding in situ measurements.

Performances of the GROC4, OC3M and two previous red-green algorithms developed for Chesapeake Bay were also compared using this dataset. The two red-green algorithms used in the comparison study were developed by Le, et al. [19] and Tzortziou, et al. [20] described in Equations (6)–(10). The algorithm developed by Le, et al. is called Red-Green Chl-a Index (hereafter RGCI) (Equations (6) and (7)), while the one developed by Tzortziou, et al. is termed the Red-Green algorithm (hereafter RG) (Equations (8)–(10)).

The RGCI algorithm [19] is:

$$\text{Chl-a} = 10^{1.76X+1.61} \tag{6}$$

where,

$$X = log_{10}\frac{R_{rs}(667)}{R_{rs}(531)} \tag{7}$$

Similarly, the RG algorithm [20] is:

$$log_{10}(Y) = 0.1725 \times log_{10}(X) - 0.5117 \tag{8}$$

where,

$$X = \text{Chl-a} \tag{9}$$

$$Y = \frac{R_{rs}(677)}{R_{rs}(554)} \tag{10}$$

To understand the seasonal performance of the GROC4 algorithm in coastal water, Chesapeake Bay's validation matchup pairs were categorized by season (Table 2): spring (March, April, May), summer (June, July, August), autumn (September, October, November) and winter (December, January, February). GROC4 derived concentrations were compared with in situ concentrations in each season.

Table 2. Summary of the matchup data used for the performance evaluation of the OC3M algorithm and GROC4 algorithm across seasons in case 2 water.

Season	Number of Samples	Chl-a (mg m^{-3})		
		Max	Min	Mean
Spring	34	29.477	1.736	10.392
Summer	29	38.021	4.410	13.109
Autumn	34	23.191	2.274	9.745
Winter	13	15.379	3.632	8.619

3. Results

Results of the performance of currently operational OC3M algorithm in deep and shallow water bodies are presented. The performance of the improved algorithm (GROC4) is also presented and compared with OC3M algorithm and that of two other existing algorithms for shallow water bodies. The seasonality and spatial trends of Chl-a in Chesapeake Bay is also estimated using GROC4 and presented.

3.1. Performance of the OC3M Algorithm in Sargasso Sea and Chesapeake Bay

When comparing the performance of the OC3M algorithm in the Sargasso Sea (case 1) and Chesapeake Bay (case 2), large differences were observed (Figures 3 and 4). For case 1 water, the coefficient of determination (r^2) obtained was 0.518 ($p < 0.001$). The spread in the scatter plot of case 1 water was low and points were mostly located along a 1:1 line whereas, the spread was quite high in the scatter plot for case 2 water (Figure 3). In Figure 3b, a vertical spread is noticeable for Chl-a concentration less than 25 mg m^{-3}. A majority of the points were above the 1:1 line suggesting that the OC3M derived concentration was overestimated in the range of 0–25 mg m^{-3}. However, beyond 25 mg m^{-3}, the OC3M model was underestimating the Chl-a concentration in case 2 water, as evident from almost all points in this range being below the 1:1 line (Figure 3b). This lack of correlation and thus accuracy in the performance of the OC3M algorithm were clearly visible in the cluster column for case 2 water and indicate that performance was concentration-dependent (Figure 4b). The cluster column for Sargasso Sea (Figure 4a) demonstrated that the OC3M derived concentrations were similar to the in situ concentrations in case 1 water, as shown by a similarity in bar heights. The measures of variation, RMSE, MAE, and MAPE show greater accuracy of the OC3M algorithm in case 1 versus case 2 water, as expected (Table 3).

Table 3. Statistics assessing accuracy of Ocean Color 3M (OC3M) derived Chl-a in Sargasso Sea (case 1) and Chesapeake Bay (case 2) water.

Water Type	Algorithm	R^2	*p*-Value	Slope	Intercept	RMSE	MAE	MAPE
Case 1	OC3M	0.518	<0.001	0.97	0.00	0.007	0.005	12.171
Case 2	OC3M	0.009	0.356	0.10	21.05	23.217	16.527	162.251

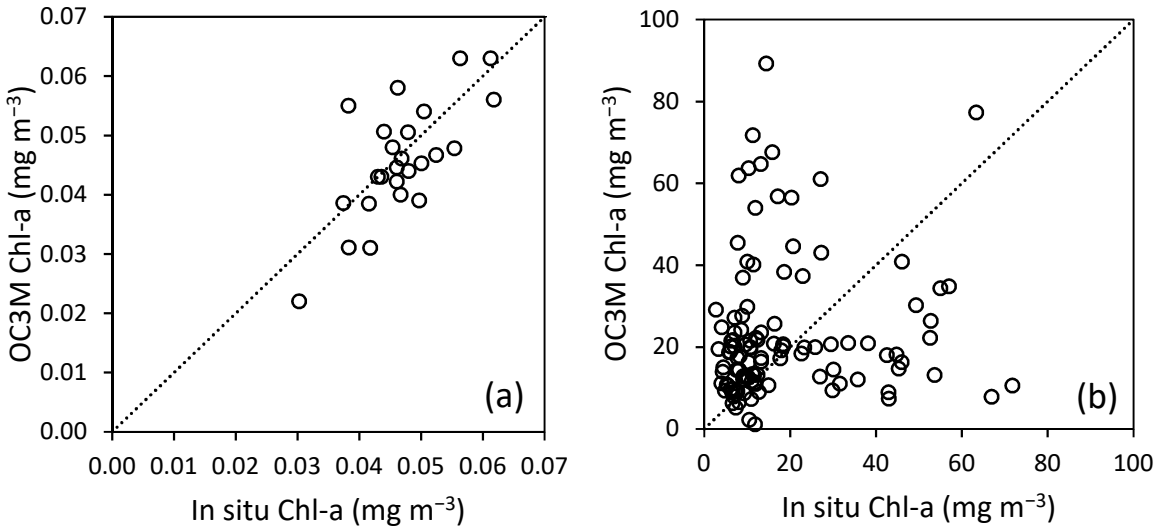

Figure 3. Scatter plots compare the OC3M derived Chl-a concentrations with in situ concentrations in (**a**) Sargasso Sea (case 1) and (**b**) Chesapeake Bay (case 2). The dotted lines represent 1:1 line.

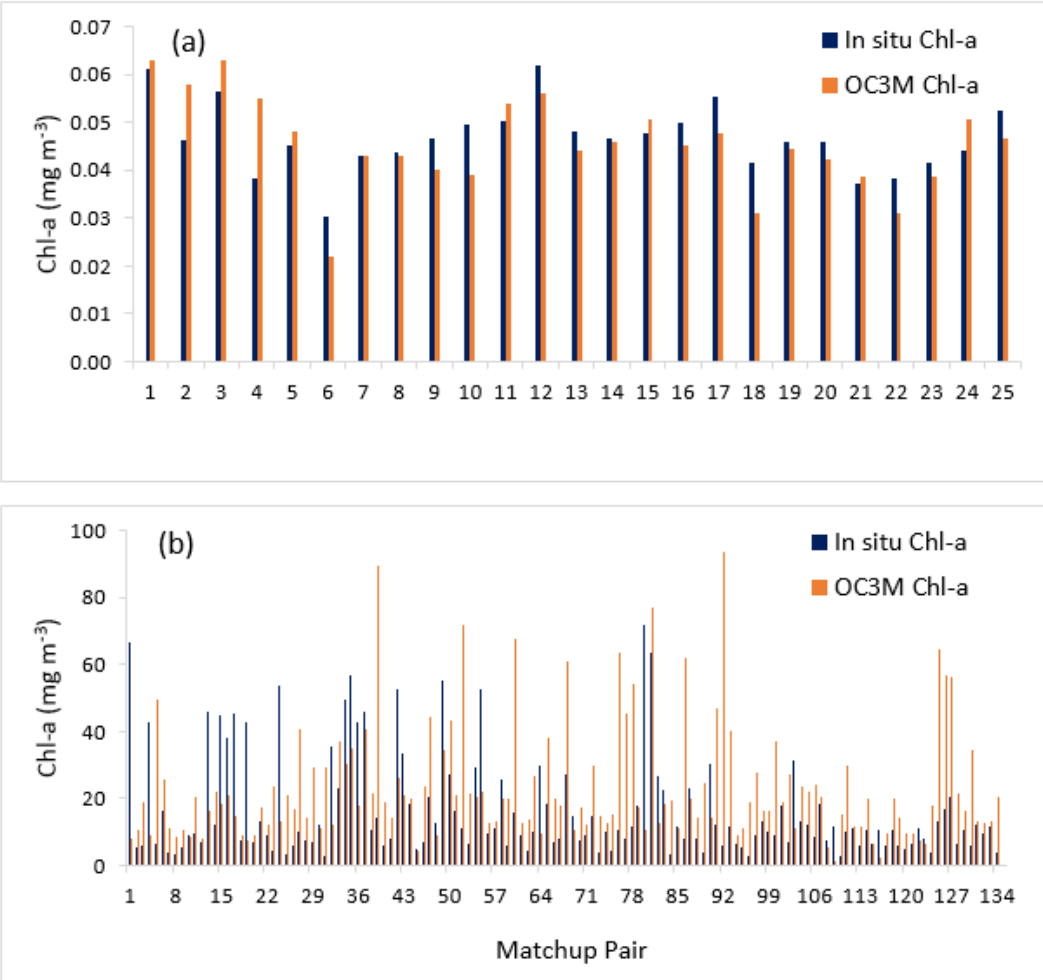

Figure 4. Clustered columns compare the OC3M algorithm derived and in situ Chl-a concentrations in (**a**) Sargasso Sea (case 1) and (**b**) Chesapeake Bay (case 2).

3.2. The GROC4 Algorithm

Since the OC3M algorithm failed to estimate Chl-a in shallow water, an improved algorithm was developed using alternative band combination. The best fit was obtained by using the reflectance ratio that employs the maximum of reflectance in 531 and 547 nm band as numerator and minimum of reflectance in 667 and 678 nm bands as the reference band. The GROC4 algorithm is described in Equations (11) and (12).

$$\text{Chl-a} = e^{a0 + a1 \times X + a2 \times X^2 + a3 \times X^3 + a4 \times X^4} \tag{11}$$

$$X = log_e \frac{\lambda_g}{\lambda_r} \tag{12}$$

where λ_g is the greater of R_{rs} at 531 and 547, and λ_r is the smaller of R_{rs} at 667 and 678. There was considerable difference in the coefficients of the OC3M algorithm compared to GROC4 algorithm (Table 4).

Table 4. Coefficients of the OC3M and GROC4 algorithms.

Algorithm	Band Ratio	Log Base	*a*0	*a*1	*a*2	*a*3	*a*4
OC3M	X_{bg}	10	0.2424	−2.7423	1.8017	0.0015	−1.2280
GROC4	X_{gr}	e	4.1579	−1.9875	−1.5994	2.1028	−0.6595

The GROC4 algorithm is a 4th order polynomial relationship between logarithmic Chl-a and green-red reflectance ratio. While the OC3M algorithm employs base-10 logarithm, the GROC4 algorithm uses the natural log. The coefficients of the GROC4 algorithm bears the same sign as OC3M algorithm, except for the quadratic term.

3.3. Validation and Comparison Analysis of the GROC4 Algorithm

The improved algorithm (GROC4), the currently-operational algorithm (OC3M), and other two prior algorithms (RGCI and RG) were compared by comparing relationships between predicted and observed Chl-a values for shallow water bodies for all four algorithms (Figure 5, Table 5).

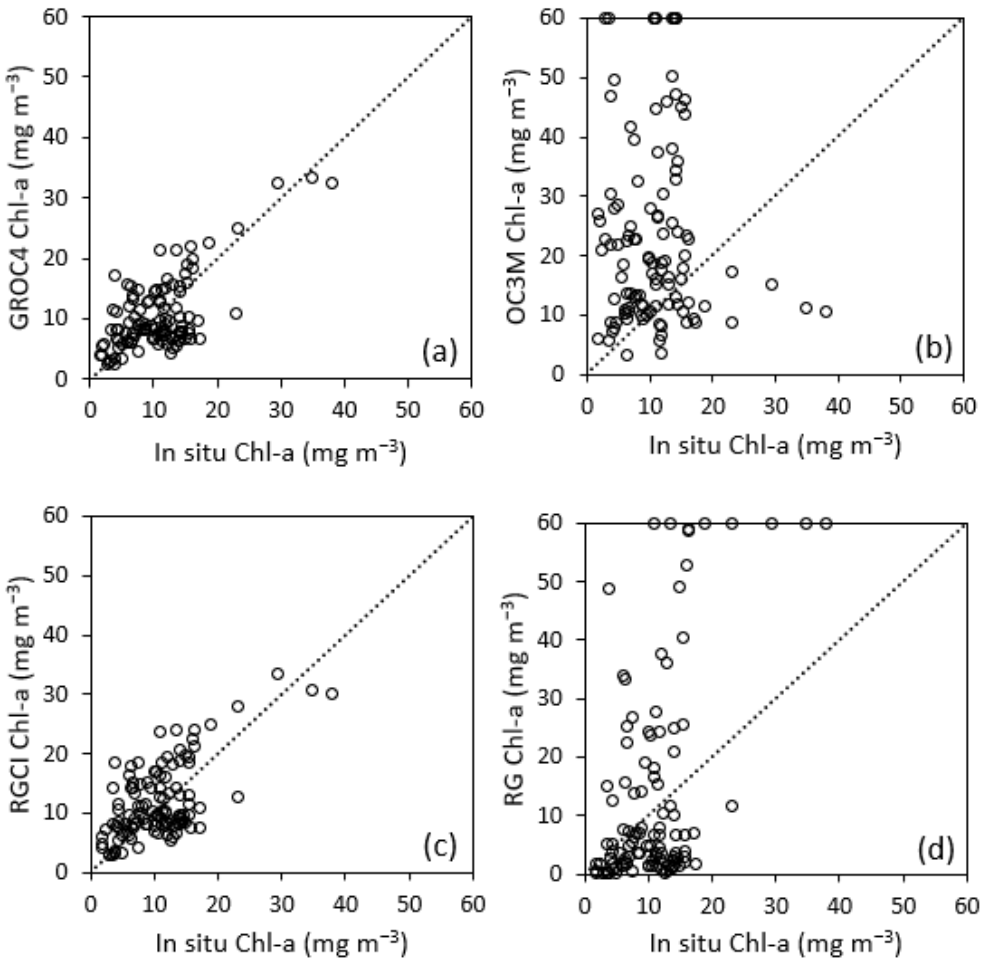

Figure 5. Scatter plots show the performance of (**a**) GROC4 (**b**) OC3M (**c**) Red-Green Chl-a Index (RGCI) and (**d**) Red-Green (RG) algorithms using the test data sample (2017). OC3M is the currently operational algorithm. while GRCI and GR are previously developed algorithms for Chesapeake Bay that use red and green bands of MODIS sensor. Dashed lines are 1:1 line. Values greater than 60 have been forced at 60 to show in the plot.

Table 5. Statistics comparing the performance of GROC4 algorithm to that of the OC3M, RGCI and RG algorithms.

Algorithm	R^2	*p*-Value	Slope	Intercept	RMSE	MAE	MAPE
GROC4	0.444	<0.001	0.67	3.29	4.924	3.921	46.401
OC3M	<0.001	0.780	−0.07	25.64	24.783	16.904	243.870
RGCI	0.405	<0.001	0.67	4.69	5.410	4.456	54.764
RG	0.495	<0.001	4.71	−30.79	37.413	17.181	132.306

The GROC4 derived Chl-a values were significantly correlated with in situ concentrations, but no relationship was observed for the OC3M-derived values (Table 5). The GROC4 algorithm also has smaller RMSE, MAE and MAPE relative to the OC3M algorithm, indicating superior performance (Table 5). For instance, the coefficient of determination for GROC4 algorithm was second highest after the RG algorithm. It should be noted that, even though the coefficient of determination of RG algorithm (0.495) was better than the GROC4 algorithm (0.444), the performance of RG algorithm was far inferior in terms of other statistical measures. The slope and intercept of the GROC4 algorithm were generally better than other algorithms except for the slope of the RGCI, which was slightly better than the GROC4 algorithm. Other than slope the statistical parameters of the GROC4 algorithm was consistently better than the RGCI algorithm whose performance was closest in comparison to the GROC4 algorithm.

3.4. Seasonal Performance of the GROC4 Algorithm

The algorithm derived and in situ concentrations for each season were analyzed to understand the seasonal performance of the GROC4 algorithm (Figure 6, Table 6). The algorithm yielded best agreement with in situ Chl-a for the summer season ($r^2 = 0.637$, $p < 0.001$), followed by the spring season ($r^2 = 0.578$, $p < 0.001$). The correlation was weak for autumn ($r^2 = 0.176$, $p = 0.014$), and statistically insignificant for winter ($r^2 = 0.067$, $p = 0.392$). Comparing other statistical measures of summer and spring, the algorithm yielded a better slope and intercept for spring whereas MAPE for summer was better than spring (Table 6). RMSE (spring = 4.685, summer = 4.644) and MAE (spring = 3.873, summer = 3.603) for the two seasons were similar. The RMSE and MAE obtained for winter were comparable to spring and summer, however the performance of the algorithm during autumn and winter appeared to be poor in terms of other statistical measures, particularly MAPE (autumn = 61.511, winter = 51.897).

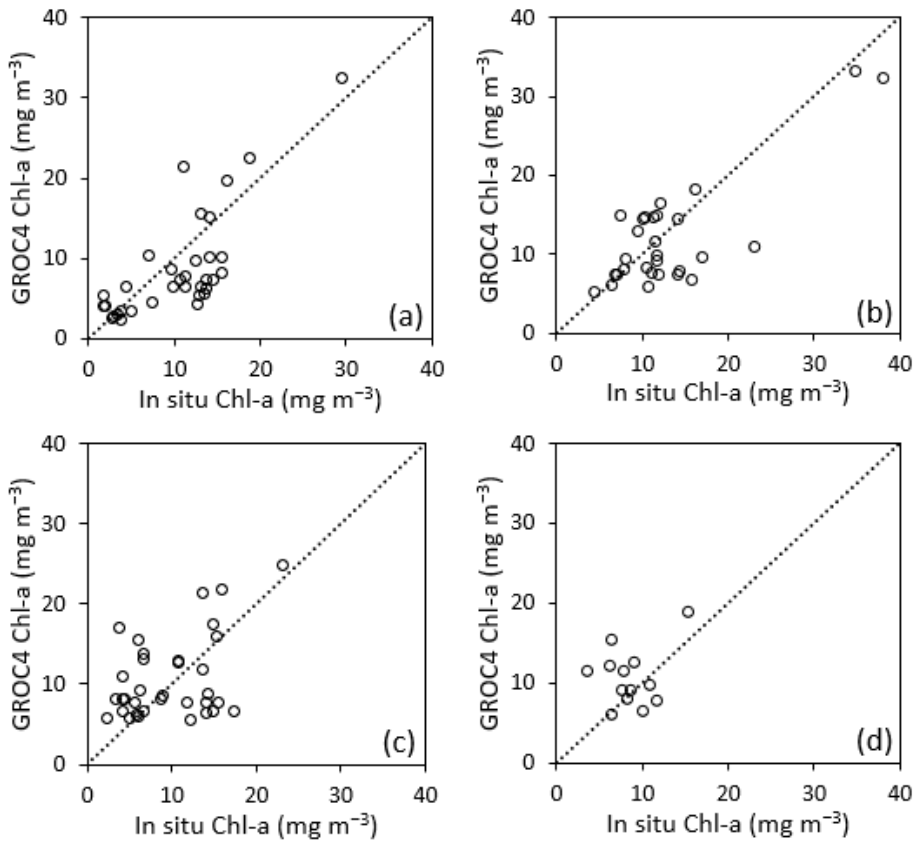

Figure 6. Seasonal comparison of in situ and GROC4 algorithm derived Chl-a in Chesapeake Bay for: (**a**) spring (**b**) summer (**c**) autumn and (**d**) winter.

Table 6. Statistics showing the seasonal performance of the GROC4 algorithm in Chesapeake Bay.

Season	R^2	*p*-Value	Slope	Intercept	RMSE	MAE	MAPE
Spring	0.578	<0.001	0.85	−0.12	4.685	3.873	44.751
Summer	0.637	<0.001	0.72	2.49	4.644	3.603	28.163
Autumn	0.176	0.014	0.42	6.57	5.546	4.424	61.511
Winter	0.067	0.392	0.32	7.93	4.387	3.439	51.897

3.5. Chl-a Map of Chesapeake Bay

A Chl-a map of Chesapeake Bay was generated by applying the GROC4 algorithm on an image acquired by MODIS Aqua, in order to analyze the spatial distribution of Chl-a in Bay waters (Figure 7). Concentrations above 25 mg m^{-3} were forced at 25 mg m^{-3} to clearly present the Chl-a pattern in the Bay water. It can be observed the spatial variability of Chl-a was significantly high in Chesapeake Bay. The concentration in the upper part of Chesapeake Bay was higher than the middle and lower part, and concentrations in tributaries were higher than those of the main channel. The concentration in a major portion of upper bay was >12.5 mg m^{-3}. The concentration in the middle and lower part was distributed more or less between 5–8 mg m^{-3} with exception of few patches. Tributaries show high concentration (~25 mg m^{-3}) at their tip, away from the main channel. Concentrations gradually dropped downstream of tributaries and became uniform with the main channel.

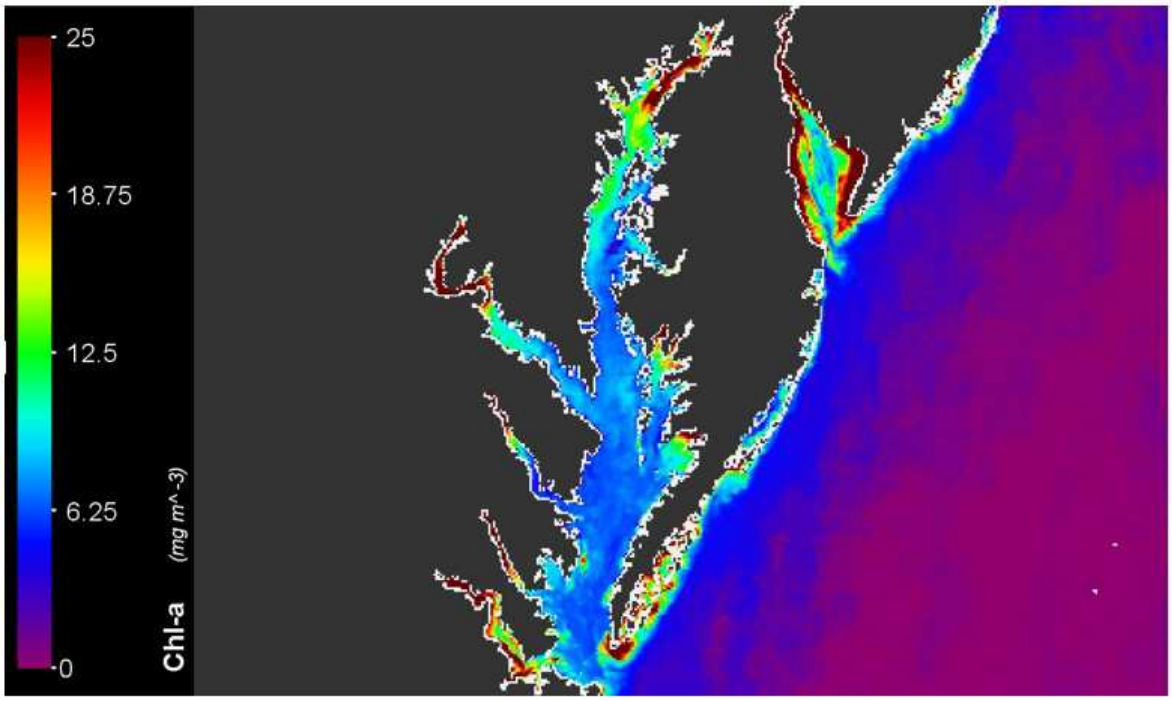

Figure 7. Example of Satellite-estimated Chl-a concentrations for Chesapeake Bay obtained by applying the GROC4 algorithm on MODIS level-2 image (dated 18 October 2017).

4. Discussion

4.1. OC3M Algorithm Performance

As in previous studies [36,37], when comparing the accuracy of OC3M algorithm in case 1 and case 2 water, we found superior performance for case 1 water. The correlation between algorithm-derived and in situ concentrations was strong for case 1 water, but non-significant for case 2 water and statistical parameters showed a better fit in case 1. The OC3M algorithm has been previously tested in other studies, including with Chesapeake Bay water [19]. The algorithm was again tested to analyze its

performance using default MODIS Aqua's level-2 data without further processing. The validation of the algorithm in Sargasso Sea provided results for comparison of the performance in case 1 and case 2 water. Our result supports the findings of previous studies that point towards good relative performance of the OC3M algorithm in deep ocean (case 1) water, and poor performance in shallow coastal water (case 2) [39,40]. Le, et al. has demonstrated a poor correlation ($r^2 < 0.16$) between blue-green band ratio and Chl-a concentration in Chesapeake Bay [19]. Zheng, et al. obtained a correlation coefficient (R) of 0.34 between MODIS Aqua derived and in situ Chl-a in Chesapeake Bay while using OC2S algorithm, a variant of OC3M algorithm [41]. While these two studies in Chesapeake Bay considered water samples collected up to a depth of 1 meter as a surface water [19,41], in the current study, samples collected at a depth of less than or equal to 0.5 meter were considered as surface water.

4.2. Performance Evaluation of the GROC4 Algorithm in Chesapeake Bay

The performance of the GROC4 algorithm is superior among the four algorithms compared in our study, although the RGCI algorithm presents a comparable result. The GROC4 algorithm performed slightly better than the RGCI algorithm for almost the whole range of Chl-a concentration, but the improvement was more evident at >20 mg m^{-3} of concentrations (Figure 5). This improvement was possibly associated with the maximum band ratio formulation of the GROC4 algorithm. Applying the observation from the mesocosm tank experiment of Schalles, et al.—i.e., with increasing Chl-a concentration the reflectance peak in the green band and trough in red band shifts towards the higher wavelength—the GROC4 algorithm was possibly able to more efficiently target the peak reflectance in the green band and trough in red band than the RGCI algorithm [14,18]. The fact that the improvement was more evident at higher concentrations further supports this hypothesis. Both GROC4 and RGCI underestimated the Chl-a concentration for most of the matchup pairs in the range of 10–20 mg m^{-3}. For the other two algorithms, OC3M overestimated for concentrations <20 mg m^{-3} and underestimated for concentrations >20 mg m^{-3}. In contrast, the RG algorithm did not show any consistent pattern, and. RG algorithm-derived concentrations were deviated from the in situ concentrations for the whole range. Even though the r-square of RG algorithm was highest among the three red-green algorithms, other statistical measures, as well as the scatter plot, showed that the algorithm was not performing well for the data set. This illustrates that a good r-square may not necessarily mean an algorithm is performing well and instead a number of statistical parameters should be considered when comparing algorithm performance.

In sum, the red-green band ratio algorithms were strongly correlated to in situ Chl-a concentrations, relative to the OC3M algorithm as depicted by coefficients of determination. This result is consistent with the finding of previous studies that have shown red band-based algorithms are less affected by noise associated with CDOM and bottom reflectance, and result in improve satellite estimation of Chl-a in coastal waters [18,42].

The GROC4 algorithm showed an improved performance over other red-NIR algorithms developed for the turbid water [23,24]. Gitelson, et al. obtained RMSE of approx. 7.9 mg m^{-3} and 8.4 mg m^{-3} using two-band model and three-band model, respectively [23]. Le, et al. obtained a RMSE of 8.68 mg m^{-3} ($r^2 = 0.48$, $p < 0.01$) for MODIS Aqua [24]. The improvement is noteworthy given the fact the GROC4 algorithm is applicable on MODIS level-2 data obtained using the standard atmospheric correction without further processing, which is required for NIR-based algorithms.

4.3. Seasonality of Chl-a

The Chl-a concentrations during spring (max = 29.477 mg m^{-3}, mean = 10.392 ± 1.012 mg m^{-3}) and summer (max = 38.021 mg m^{-3}, mean = 13.109 ± 1.366 mg m^{-3}) were higher than autumn (max = 23.191 mg m^{-3}, mean = 9.745 ± 0.869 mg m^{-3}) and winter (max = 15.379 mg m^{-3}, mean = 8.619 ± 0.785) (Table 2). Even though mean concentrations are comparable across seasons, samples with high Chl-a concentration were present in spring and summer data set as evident from the maximum Chl-a concentration for each season. The better estimation by the algorithm at

higher concentration than at lower concentration might explain the better seasonal performance of the GROC4 algorithm during spring and summer. The strong correlation for summer (Figure 6b) is a function of the contribution of two observations with high Chl-a concentrations (>30 mg m^{-3}) where the algorithm appears to perform well. It should be noted that spring and summer are important seasons in Chesapeake Bay in terms of Chl-a monitoring. Spring phytoplankton blooms are a seasonal phenomenon in Chesapeake Bay that results in high Chl-a concentrations across Bay waters [43]. Generally, the Chl-a concentrations during summer are less than in spring [43]. The organic materials deposited during spring decompose during summer which renders the bottom water anoxic or hypoxic [43]. An extended duration of bloom condition during spring then has implications for water quality during summer. Therefore, monitoring Chl-a during spring and summer, and in the transitional period is an important aspect of Chesapeake Bay ecological management. Therefore, even with the poor performance during autumn and winter, a strong correlation during spring and summer bolsters the potential benefits of this algorithm.

4.4. Spatial Map of Chl-a

The Susquehanna river drains a large amount of nutrients in the upper bay [28,44]. The excess availability of nutrient in the upper bay could explain the high concentration of Chl-a in this region. Other rivers, such as Potomac, Rappahannock etc. drain in mid and lower bay, but it should be noted Susquehanna river alone drains about 50% of the fresh water of the whole estuary, contributing 66% of nitrogen and 40% of the phosphorus input [28,45]. The Chl-a concentration in the mid bay and lower bay might not be influenced by nutrient loading from the Susquehanna River due to long travel distance and the tidal mixing of water.

The enhanced performance depicted by the GROC4 algorithm over other algorithms tested in this study, especially OC3M algorithm, encourages its application for Chl-a monitoring in Chesapeake Bay. Together with MODIS Aqua data, it can be used to track Chl-a variability in the Bay water, especially in those sections where Chl-a concentrations remain high and therefore need more attention. A limitation of MODIS Aqua sensor is that due to its low spatial resolution (1 km), it does not capture data close to land boundaries (white patches along land-water boundaries). Thus, Chl-a concentration near the coastline and in the narrow tributaries could not be determined using remote sensing data from the sensor.

5. Conclusions

In this study, the performance of the OC3M algorithm was assessed across the deep ocean and a coastal water body. An improved algorithm was developed based on reflectance data from the green and red bands and its performance in the coastal water system of Chesapeake Bay was tested using an independent dataset. The OC3M algorithm worked well for case 1 water. However, the error of estimation was very high in case 2 waters. The result of this analysis demonstrates that OC3M algorithm is useful for synoptic mapping of Chl a in the deep ocean region. However, the high error of estimation in Chesapeake Bay shows that the algorithm is unsuitable for satellite estimation of Chl-a in coastal waters.

The present study also demonstrated the usefulness of maximum-green-red band ratio formulation for Chl a estimation in complex coastal water. The GROC4 algorithm performed significantly better than the OC3M algorithm in the coastal water of Chesapeake Bay. The RMSE was reduced from of 24.783 mg m^{-3} to 4.924 mg m^{-3} when the GROC4 algorithm was used instead of the OC3M algorithm for the same validation dataset. The evaluation of seasonal performance of the algorithm demonstrated that the GROC4 algorithm is significantly correlated with Chl-a during spring and summer.

The implementation of the algorithm developed in this study is simple and requires only reflectance data in wavebands that are available from MODIS Aqua sensor. It could be used to understand the dynamics of Chl-a in coastal water by using the long record of publicly available MODIS Aqua ocean color data. Although, GROC4 algorithm reduced the error in deriving Chl-a by a significant margin,

the following limitations remain. The matchup dataset used for the development of the algorithm is small (134 pairs). For most of the pixels in the MODIS imagery of the study area, reflectance data is not available, and frequency of in situ observations is low. It would be better to utilize a larger set of matchup pixels in order to develop an algorithm with a greater accuracy. Furthermore, the satellite estimation of Chl-a in coastal water is severely affected by the operational atmospheric correction procedures that are known to be inefficient [46]. Therefore, an encouraging prospect for enhancement in satellite estimation of Chl-a in coastal water is improvement in atmospheric correction procedure and development of an algorithm using the maximum green-red band ratio with a larger set of matchup pixels.

This study addresses the important issue of coastal water algal bloom mapping [47] using satellite data with reasonable accuracy, and showed an improvement over the existing operational algorithm. The results of this study can be applicable to water bodies and can lead to further improvements in as algorithm performance.

Author Contributions: Conceptualization, M.M.A., A.M.M. and L.J.S.; Methodology, M.M.A. and A.M.M.; Software, M.M.A. and A.M.M.; Validation, M.M.A.; Formal Analysis, M.M.A. and A.M.M.; Investigation, M.M.A. and A.M.M.; Resources, M.M.A., L.J.S., J.S.R. and A.M.M.; Data Curation, M.M.A. and A.M.M.; Writing-Original Draft Preparation, M.M.A., L.J.S., J.S.R. and A.M.M.; Writing-Review & Editing, M.M.A., L.J.S., J.S.R. and A.M.M.; Visualization, M.M.A., A.M.M.; Supervision, A.M.M., L.J.S. and J.S.R.; Project Administration, A.M.M.; Funding Acquisition, M.M.A. and A.M.M.

Funding: This research received no external funding. The first author received funding from the Department of Earth and Environment, Florida International University for his graduate studies during this study.

Acknowledgments: The authors would like to thank the Ocean Biology Processing Group (OBPG), NASA Goddard Space Flight Centre for Ocean Color data. Thanks are also due to Chesapeake Bay Program (CBP) and National Centers for Environmental Information. We would like to acknowledge also the Department of Earth and Environment for the graduate assistantship provided for the first author during this study. This study was developed in collaboration with the National Science Foundation Florida Coastal Everglades Long Term Ecological program under Grant #DEB-1237517. This is contribution #914 from the Southeast Environmental Research Center in the Institute of Water and Environment at Florida International University.

Conflicts of Interest: The authors declare no conflict of interest.

References

1. Van Dolah, F.M. Marine algal toxins: Origins, health effects, and their increased occurrence. *Environ. Health Perspect.* **2000**, *108* (Suppl. 1), 133–141. [CrossRef] [PubMed]
2. Pierce, R.H.; Henry, M. Harmful algal toxins of the Florida red tide (Karenia brevis): Natural chemical stressors in South Florida coastal ecosystems. *Ecotoxicology* **2008**, *17*, 623–631. [CrossRef] [PubMed]
3. Pinckney, J.L.; Paerl, H.W.; Tester, P.; Richardson, T.L. The role of nutrient loading and eutrophication in estuarine ecology. *Environ. Health Perspect.* **2001**, *109* (Suppl. 5), 699–706. [PubMed]
4. Smith, V.H. Eutrophication of freshwater and coastal marine ecosystems a global problem. *Environ. Sci. Pollut. Res.* **2003**, *10*, 126–139. [CrossRef]
5. Moore, S.K.; Trainer, V.L.; Mantua, N.J.; Parker, M.S.; Laws, E.A.; Backer, L.C.; Fleming, L.E. Impacts of climate variability and future climate change on harmful algal blooms and human health. *Environ. Health* **2008**, *7* (Suppl. 2), S4. [CrossRef]
6. Mélin, F.; Hoepffner, N. Monitoring Phytoplankton Productivity from Satellite—An Aid to Marine Resources Management. In *Handbook of Satellite Remote Sensing Image Interpretation: Applications for Marine Living Resources Conservation and Management*; Morales, J., Stuart, V., Platt, T., Sathyendranath, S., Eds.; EU PRESPO and IOCCG, 2011; pp. 79–93. Available online: https://www.ioccg.org/handbook/casestudy6_melin_hoepffner.pdf (accessed on 6 August 2019).
7. Cullen, J.J. The deep chlorophyll maximum: Comparing vertical profiles of chlorophyll. *Can. J. Fish. Aquat. Sci.* **1982**, *39*, 791–803. [CrossRef]
8. Dore, J.E.; Letelier, R.M.; Church, M.J.; Lukas, R.; Karl, D.M. Summer phytoplankton blooms in the oligotrophic North Pacific Subtropical Gyre: Historical perspective and recent observations. *Prog. Oceanogr.* **2008**, *76*, 2–38. [CrossRef]

9. Joint, I.; Groom, S.B. Estimation of phytoplankton production from space: Current status and future potential of satellite remote sensing. *J. Exp. Mar. Biol. Ecol.* **2000**, *250*, 233–255. [CrossRef]
10. O'Reilly, J.E.; Maritorena, S.; Mitchell, B.G.; Siegel, D.A.; Carder, K.L.; Garver, S.A.; Kahru, M.; McClain, C. Ocean color chlorophyll algorithms for SeaWiFS. *J. Geophys. Res. Ocean.* **1998**, *103*, 24937–24953.
11. Blondeau-Patissier, D.; Gower, J.F.R.; Dekker, A.G.; Phinn, S.R.; Brando, V.E. A review of ocean color remote sensing methods and statistical techniques for the detection, mapping and analysis of phytoplankton blooms in coastal and open oceans. *Prog. Oceanogr.* **2014**, *123*, 123–144. [CrossRef]
12. Darecki, M.; Stramski, D. An evaluation of MODIS and SeaWiFS bio-optical algorithms in the Baltic Sea. *Remote Sens. Environ.* **2004**, *89*, 326–350. [CrossRef]
13. Morel, A.; Prieur, L. Analysis of variations in ocean color 1. *Limnol. Oceanogr.* **1977**, *22*, 709–722. [CrossRef]
14. Schalles, J.F. Optical remote sensing techniques to estimate phytoplankton chlorophyll a concentrations in coastal. In *Remote Sensing of Aquatic Coastal Ecosystem Processes*; Springer: Dordrecht, The Netherlands, 2006; pp. 27–79.
15. Carder, K.L.; Cannizzaro, J.P.; Lee, Z. Ocean color algorithms in optically shallow waters: Limitations and improvements. In *Remote Sensing of the Coastal Oceanic Environment*; International Society for Optics and Photonics: Bellingham, WA, USA, 2005.
16. Moses, W.J.; Gitelson, A.A.; Berdnikov, S.; Povazhnyy, V. Estimation of chlorophyll-a concentration in case II waters using MODIS and MERIS data—Successes and challenges. *Environ. Res. Lett.* **2009**, *4*, 045005. [CrossRef]
17. Richardson, L.L.; LeDrew, E.F. *Remote Sensing of Aquatic Coastal Ecosystem Processes*; Springer: Dordrecht, The Netherlands, 2006.
18. Gilerson, A.A.; Gitelson, A.A.; Zhou, J.; Gurlin, D.; Moses, W.; Ioannou, I.; Ahmed, S.A. Algorithms for remote estimation of chlorophyll-a in coastal and inland waters using red and near infrared bands. *Opt. Express* **2010**, *18*, 24109–24125. [CrossRef] [PubMed]
19. Le, C.; Hu, C.; Cannizzaro, J.; Duan, H. Long-term distribution patterns of remotely sensed water quality parameters in Chesapeake Bay. *Estuar. Coast. Shelf Sci.* **2013**, *128*, 93–103. [CrossRef]
20. Tzortziou, M.; Subramaniam, A.; Herman, J.R.; Gallegos, C.L.; Neale, P.J.; Harding, L.W., Jr. Remote sensing reflectance and inherent optical properties in the mid Chesapeake Bay. *Estuar. Coast. Shelf Sci.* **2007**, *72*, 16–32. [CrossRef]
21. Le, C.; Hu, C.; English, D.; Cannizzaro, J.; Chen, Z.; Feng, L.; Boler, R.; Kovach, C. Towards a long-term chlorophyll-a data record in a turbid estuary using MODIS observations. *Prog. Oceanogr.* **2013**, *109*, 90–103. [CrossRef]
22. Gons, H.J.; Rijkeboer, M.; Ruddick, K.G. A chlorophyll-retrieval algorithm for satellite imagery (Medium Resolution Imaging Spectrometer) of inland and coastal waters. *J. Plankton Res.* **2002**, *24*, 947–951. [CrossRef]
23. Gitelson, A.A.; Schalles, J.F.; Hladik, C.M. Remote chlorophyll-a retrieval in turbid, productive estuaries: Chesapeake Bay case study. *Remote Sens. Environ.* **2007**, *109*, 464–472. [CrossRef]
24. Le, C.; Hu, C.; Cannizzaro, J.; English, D.; Muller-Karger, F.; Lee, Z. Evaluation of chlorophyll-a remote sensing algorithms for an optically complex estuary. *Remote Sens. Environ.* **2013**, *129*, 75–89. [CrossRef]
25. Blakey, T.; Melesse, A.; Sukop, M.C.; Tachiev, G.; Whitman, D.; Miralles-Wilhelm, F. Developing Benthic Class Specific, Chlorophyll-a Retrieving Algorithms for Optically-Shallow Water Using SeaWiFS. *Sensors* **2016**, *16*, 1749. [CrossRef] [PubMed]
26. Powledge, F. Chesapeake bay restoration: A model of what? *BioScience* **2005**, *55*, 1032–1038. [CrossRef]
27. Ator, S.W.; Denver, J.M. *Understanding the Nutrients in the Chesapeake Bay Watershed and Implications for Management and Restoration: The Eastern Shore*; US Geological Survey: Reston, VA, USA, 2015.
28. Ator, S.W.; Brakebill, J.W.; Blomquist, J.D. *Sources, Fate, and Transport of Nitrogen and Phosphorus in the Chesapeake Bay Watershed: An Empirical Model*; US Geological Survey: Reston, VA, USA, 2011; Volume 5167.
29. Ha, N.; Koike, K.; Nhuan, M. Improved accuracy of chlorophyll-a concentration estimates from MODIS imagery using a two-band ratio algorithm and geostatistics: As applied to the monitoring of eutrophication processes over Tien Yen Bay (Northern Vietnam). *Remote Sens.* **2013**, *6*, 421–442. [CrossRef]
30. Son, S.; Wang, M. Water properties in Chesapeake Bay from MODIS-Aqua measurements. *Remote Sens. Environ.* **2012**, *123*, 163–174. [CrossRef]

31. Ryberg, K.R.; Blomquist, J.D.; Sprague, L.A.; Sekellick, A.J.; Keisman, J. Modeling drivers of phosphorus loads in Chesapeake Bay tributaries and inferences about long-term change. *Sci. Total Environ.* **2018**, *616*, 1423–1430. [CrossRef]
32. Freestone, D.; Bulger, F. The Sargasso Sea commission: An innovative approach to the conservation of areas beyond national jurisdiction. *Ocean Yearb.* **2016**, *30*, 80–90.
33. Morel, A.; Claustre, H.; Gentili, B. The most oligotrophic subtropical zones of the global ocean: Similarities and differences in terms of chlorophyll and yellow substance. *Biogeosciences* **2010**, *7*, 3139–3151. [CrossRef]
34. Mackey, K.R.M.; Buck, K.N.; Casey, J.R.; Cid, A.; Lomas, M.W.; Sohrin, Y.; Paytan, A. Phytoplankton responses to atmospheric metal deposition in the coastal and open-ocean Sargasso Sea. *Front. Microbiol.* **2012**, *3*, 359. [CrossRef]
35. Chesapeake Bay Program. Chesapeake Bay Program Water Quality Database 1984–Present. Available online: http://www.chesapeakebay.net/data/downloads/cbp_water_quality_database_1984_present (accessed on 20 December 2018).
36. National Centers for Environmental Information. Available online: https://www.nodc.noaa.gov/archive/arc0030/0067471/1.1/data/ (accessed on 15 April 2018).
37. NASA Goddard Space Flight Center, Ocean Ecology Laboratory, Ocean Biology Processing Group. Moderate-Resolution Imaging Spectroradiometer (MODIS) Aqua Ocean Color Data. 2018. Available online: https://oceancolor.gsfc.nasa.gov/ (accessed on 6 August 2019).
38. Bailey, S.W.; Werdell, P.J. A multi-sensor approach for the on-orbit validation of ocean color satellite data products. *Remote Sens. Environ.* **2006**, *102*, 12–23. [CrossRef]
39. Hattab, T.; Jamet, C.; Sammari, C.; Lahbib, S. Validation of chlorophyll-α concentration maps from Aqua MODIS over the Gulf of Gabes (Tunisia): Comparison between MedOC3 and OC3M bio-optical algorithms. *Int. J. Remote Sens.* **2013**, *34*, 7163–7177. [CrossRef]
40. Minu, P.; Lotliker, A.A.; Shaju, S.S.; Ashraf, P.M.; Kumar, T.S.; Meenakumari, B. Performance of operational satellite bio-optical algorithms in different water types in the southeastern Arabian Sea. *Oceanologia* **2016**, *58*, 317–326. [CrossRef]
41. Zheng, G.; DiGiacomo, P.M. Remote sensing of chlorophyll-a in coastal waters based on the light absorption coefficient of phytoplankton. *Remote Sens. Environ.* **2017**, *201*, 331–341. [CrossRef]
42. Ha, N.T.T.; Thao, N.T.P.; Koike, K.; Nhuan, M.T. Selecting the Best Band Ratio to Estimate Chlorophyll-a Concentration in a Tropical Freshwater Lake Using Sentinel 2A Images from a Case Study of Lake Ba Be (Northern Vietnam). *ISPRS Int. J. Geo-Inf.* **2017**, *6*, 290. [CrossRef]
43. Cerco, C.F. Phytoplankton kinetics in the Chesapeake Bay eutrophication model. *Water Qual. Ecosyst. Model.* **2000**, *1*, 5–49. [CrossRef]
44. Harding, L.W.; Mallonee, M.E.; Perry, E.S.; Miller, W.D.; Adolf, J.E.; Gallegos, C.L.; Paerl, H.W. Long-term trends, current status, and transitions of water quality in Chesapeake Bay. *Sci. Rep.* **2019**, *9*, 6709. [CrossRef]
45. Langland, M.J.; Hainly, R.A. *Changes IN Bottom-Surface Elevations IN Three Reservoirs on the Lower Susquehanna River, Pennsylvania and Maryland, Following the January 1996 Flood; Implications for Nutrient and Sediment Loads to Chesapeake Bay*; US Geological Survey: Reston, VA, USA, 1997.
46. Wang, S.; Li, J.; Zhang, B.; Shen, Q.; Zhang, F.; Lu, Z. A simple correction method for the MODIS surface reflectance product over typical inland waters in China. *Int. J. Remote Sens.* **2016**, *37*, 6076–6096.
47. Shen, L.; Xu, H.; Guo, X. Satellite remote sensing of harmful algal blooms (HABs) and a potential synthesized framework. *Sensors* **2012**, *12*, 7778–7803. [CrossRef]

© 2019 by the authors. Licensee MDPI, Basel, Switzerland. This article is an open access article distributed under the terms and conditions of the Creative Commons Attribution (CC BY) license (http://creativecommons.org/licenses/by/4.0/).